



Nominate a Worthy Chemist Chemistry Europe Award

Subject:

chemistry for sustainability,
energy, materials,
environment

Consists of:

prize money amounting to
EUR 10,000, certificate

Deadline:

November 1, 2022



**Click here for more
info & nomination**

Materials Science inc. Nanomaterials & Polymers

Bisphosphonates on Smooth TiO₂: Modeling and CharacterizationLeonardo F. G. Dias,^{*[a, b]} João P. C. Rheinheimer,^[b] Orisson P. Gomes,^[b] Michael Noeske,^[a] Stephani Stamboroski,^[a, c] Erika S. Bronze-Uhle,^[d] Maria C. Mainardi,^[a] Welchy L. Cavalcanti,^[a] Augusto B. Neto,^[e] and Paulo N. Lisboa-Filho^[b]

This paper presents insights into surfaces properties of sputter-deposited titania modified with bisphosphonates, including zeta potential measurements in a pH range. Functionalization was investigated through simulation and experimental approaches to model the adsorbate and evaluate structure-response relationships. Molecules of etidronic, alendronic, and risedronic acids were investigated through density functional theory. The molecules vary their reactivity through similar structures considering different scenarios. X-ray photoelectron spectroscopy of titania/BP systems demonstrated that function-

alization occurs in a short time and resulted in a predominantly "side-on" adsorbate configuration after two hours of immersion. Zeta potential showed the predominancy of negative charges deprotonated free phosphonates. Water contact angle demonstrated that titania surfaces are hydrophilic after overnight functionalization. Atomic force measurements of bisphosphonates layers suggested that the molecular anions follow the surface topography, unchanging the surface roughness.

Introduction

Bisphosphonates (BPs) are molecular anions of organic molecules analogous to pyrophosphate.^[1] Unlike pyrophosphate, BPs have a central carbon that allows the presence of two substituents (R₁ and R₂), as shown in Figure 1.^[2] The substituent R₁ is in general a hydroxyl group, and R₂ can vary from a methyl

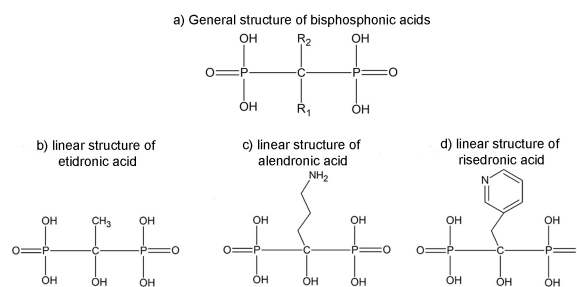


Figure 1. a) General structure of bisphosphonic acids and linear structure of b) etidronic acid, c) alendronic acid and d) risedronic acid.

to a nitrogen-containing heterocyclic ring. Such groups play an essential role in the biological activity of these molecules. A nitrogen-containing bisphosphonate can have a 10000 times more potent osteogenic effect than a BP containing only a methyl group.^[3] This work chooses etidronic acid, alendronic acid, and risedronic acid as surfaces modifiers. These anions were considered since etidronic acid is the simplest structure for bisphosphonic acid, while alendronic and risedronic acid are nitrogen-containing BP, with a linear and cyclic nitrogen, respectively. Thus, these three molecules cover a variety of bisphosphonic acids structure.

Although BPs have been intensely studied throughout the years, some points still need to be clarified about their pharmacological functions and their potential as surface modifiers.^[4,5] Frequently, the BPs are adsorbed on or combined with hydroxyapatite (HA), because such molecular anions have a strong affinity for HA surfaces and can coordinate Ca²⁺,^[6] to increase cell growth and proliferation of implants surfaces.

[a] L. F. G. Dias, Dr. M. Noeske, S. Stamboroski, Prof. M. C. Mainardi, Dr. W. L. Cavalcanti
Fraunhofer Institute for Manufacturing Technology and Advanced Materials IFAM
Wiener Straße, 28359 Bremen, Germany
E-mail: goncalves.dias@unesp.br

[b] L. F. G. Dias, J. P. C. Rheinheimer, O. P. Gomes, P. N. Lisboa-Filho
São Paulo State University - UNESP,
School of Science, Bauru, Brazil
Av. Eng. Luís Edmundo Carrijo Coube, 14-01 – Nucleo Res. Pres. Geisel,
Bauru - SP, 17033-360

[c] S. Stamboroski
University of Bremen, Otto-Hahn-Allee 1,
28359 Bremen, Germany

[d] Dr. E. S. Bronze-Uhle
Bauru School of Dentistry, Sao Paulo University – USP,
Bauru, SP, Brazil
Alameda Dr. Octávio Pinheiro Brisolla, 9-75 – Vila Regina,
Bauru – SP, 17012-230

[e] Prof. A. B. Neto
Sao Paulo State University - UNESP, Campus of Itapeva, Itapeva, SP, Brazil
R. da Pátria, 519 - Vila Nossa Sra. de Fatima,
Itapeva – SP, 18409-010

Supporting information for this article is available on the WWW under <https://doi.org/10.1002/slct.202200286>

© 2022 The Authors. ChemistrySelect published by Wiley-VCH GmbH. This is an open access article under the terms of the Creative Commons Attribution License, which permits use, distribution and reproduction in any medium, provided the original work is properly cited.

Regardless of their attested biocompatibility, the production of HA surfaces is laborious, mainly on metallic substrates such as titanium alloys used as implants, screws, and plates, exhibiting a poor adhesion between film and substrate.^[7,8] To avoid complications related to the film-substrate interface, the use of titanium dioxide films is a solution to explore the entire potential of immobilized bisphosphonates. Different studies present the properties of TiO₂, such as biocompatibility, corrosion resistance, and presence of hydroxyl groups, suitable characteristics for an implant cover.^[9–11]

As surfaces modifiers, most studies with bisphosphonates have focused only on the biological aspects. Thus, there is a lack of information about the effects of BPs adsorption on metallic and oxidized surfaces. For example, surface energy and groups previously adsorbed on the titania surface modify the interaction between the substrate and the molecules.^[12,13]

Through an X-ray photoelectron spectroscopy (XPS) and density functional theory (DFT), it was demonstrated that titanium implants functionalized with alendronate exhibit decreased contact angle. In addition, competitive adsorption takes place between two configurations: the first conformation amino (–NH₂) and phosphonic acid (–PO₃H₂) groups bound on the surface; the second occurs through phosphonic acid (–PO₃H₂) groups only.^[14] Despite using different techniques, the influence of roughness was not mentioned in the referred study, as only one bisphosphonate was used and simulated in a vacuum.

Hence, in this work, we demonstrated the modification of surface properties caused by bisphosphonates' adsorption on smooth titanium dioxide. The choice of this specific substrate is due to its common application as an implant cover.^[15] The proposed approach was applied with the same substrate using quaternary ammonium-containing silane and octadecyl phosphonic acid (ODPA), which demonstrated the association between biological activity and layer structure.^[16] The use of a smooth substrate aims to reduce the influence of the geometric surface area, which can increase the surface charge or even the interaction between layers and cells.^[17–19]

In this work, bisphosphonic acids were simulated using density functional theory (DFT) to predict their properties. Different studies used DFT to explore the adsorption of BPs. Such an approach provides the HOMOs (highest occupied molecular orbital), the LUMOs (lowest occupied molecular orbital), and the density of states, permitting the most reactive sites of the BPs to be found. Few works have considered that the molecules display different protonation and deprotonation states with the pH – important for adsorption experiments – and most of them focused on the adsorption on hydroxyapatite crystals.^[2,20,21] However, TiO₂ is also employed as an implant coating.

In this way, the performed simulations considered the different states of protonation and deprotonation, and these results were compared with X-ray photoelectron spectroscopy providing aspects of BPs adsorption. The results were complemented with water contact angle (WCA), zeta potential, and atomic force microscopy (AFM) measurements. XPS evaluated short-time immersion (2 h) and long-time immersion (24 h),

samples were analyzed through other techniques, XPS investigations of overnight immersion were published elsewhere.^[13]

Results and Discussion

Theoretical modeling

A reactivity study of distinctly protonated bisphosphonic acids in an aqueous solution in contact with uncharged crystalline titania surfaces was conducted to investigate whether the reactive regions are consistent with typical adsorption centers of the BP-based entities on the substrates. As BP structures are very susceptible to pH influence, molecules or ions were simulated in different protonation and deprotonation states. In pH 7, etidronic acid can undergo two or three deprotonations.^[20] Alendronate passes through one protonation and two deprotonations.^[20,22] On the other hand, risedronate undergoes two or three deprotonations.^[23] Information regarding theoretical modeling in vacuum and water for neutral bisphosphonates is available in the supplementary material.

Figure 2 exhibits the DFT results for the BP structures simulated in a water environment. In this figure, blue and red colors are both related to CAFI/MEP results and indicate positively and negatively charged sites, respectively. According to the presented RGB scale, the other colors indicate regions with intermediate charge concentration. As the protonation/deprotonation state causes an unbalance in the total charge of the molecule, it becomes impossible to use a single value scale for the MEP results. For this reason, each molecule has asterisks (*) that indicate the exact numeric scale used for the MEP results.

In general, CAFI indicates interactions involving the frontier orbitals of nucleophilic (f^+) and electrophilic (f^-) species. Such interactions are commonly defined as “soft-soft” interactions since they are associated with deformations in the frontier orbitals induced by external species, while MEP shows possible electrostatic interactions, known as “hard-hard” interactions with little deformation of the electronic molecular orbital.^[24]

In etidronic acid with two deprotonations (ETI-2DP), the –OH of the phosphonic acid group is the region more susceptible to nucleophilic attacks, while the phosphonic acid group and the –OH are the regions more prone to interact with external electrophilic sites. The MEP of etidronate displays regions of elevated negative electrostatic potential around the oxygen atoms of the molecule, while the positive electrostatic potential regions remain around the H atoms.

For the etidronate with three deprotonations (ETI-3DP), the –OH group of the phosphonic acid that did not deprotonate presented a reactive site related to nucleophilic attacks, which can indicate that the etidronic acid could go through four deprotonations. For electrophilic attacks, the phosphonic acid group that passed through three deprotonations on –OH showed to be the most probable region to interact with electrophilic agents. The MEP displays regions of intense negative electrostatic potential around the deprotonated oxygen atoms of the phosphonate groups, while the regions of

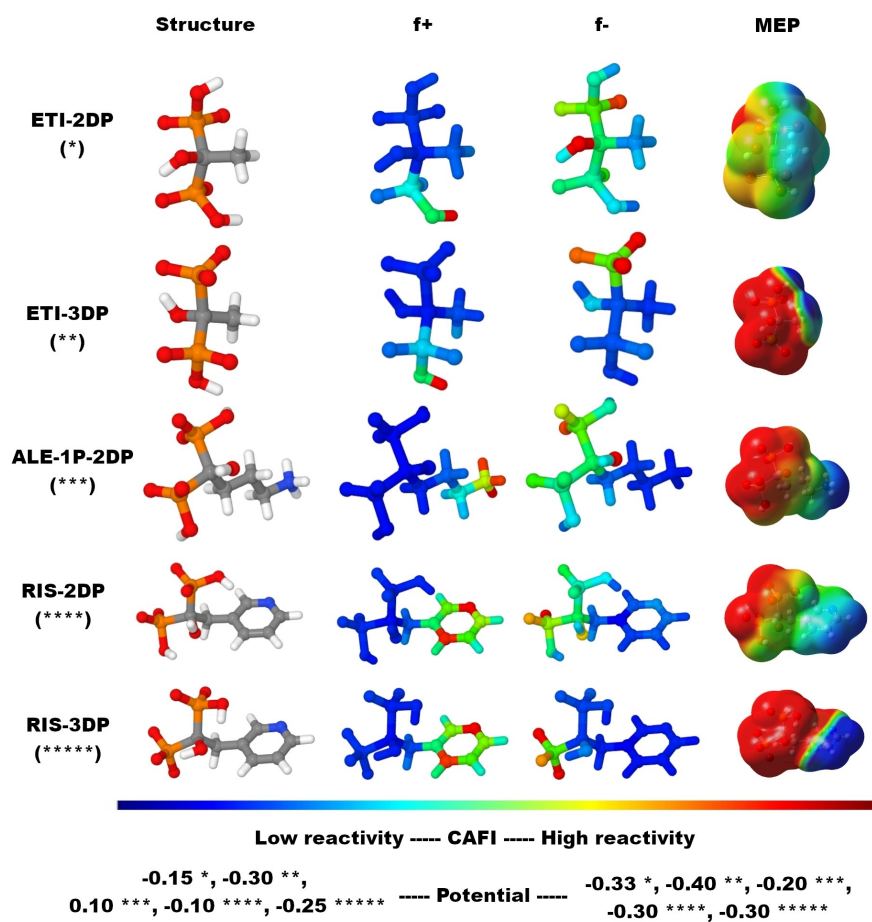


Figure 2. Structure, Fukui indices, and map of electrostatic potential (MEP) of studied molecules when dissolved in water. The number of asterisks (*) in each molecule is used to indicate the scale of the electrostatic potential map because the protonated/deprotonated states of the molecule are unbalanced in the charge.

positive electrostatic potential remain around the hydrogen atoms that were not deprotonated.

In alendronate with one protonation and two deprotonations (ALE-1P-2DP), the region more prone to interact with external nucleophilic attacks is the $-\text{NH}_3$. For external electrophilic attacks, the reactivity of the molecule concentrates around the phosphonic acid group, mainly in the deprotonated oxygen atom. The MEP displays regions of negative electrostatic potential around the phosphonate groups, while the region of positive electrostatic potential remains in the amine group.

The risedronate with two deprotonations (RIS-2DP) exhibits a region prone to interact with nucleophilic attacks around the pyridine ring, especially for the nitrogen atom. For electrophilic attacks, the more prone regions are the phosphonic acid groups, mainly in the deprotonated oxygen atom. The MEP shows regions of negative electrostatic potential around the phosphonic acid group and regions of positive electrostatic potential around the pyridine ring.

For the risedronate with three deprotonations (RIS-3DP), the reactivity for nucleophilic attacks remains as in risedronate

with two deprotonations (RIS-2DP), concentrated in the pyridine ring (mainly in the nitrogen atom and in its position). The regions are inclined to interact with external electrophilic attacks concentrated in the phosphonic acid group with all oxygen atoms deprotonated. The MEP displays regions of negative electrostatic potential around the phosphonic acid groups, while the negative electrostatic potential regions are more present around the pyridine ring.

Such results are consistent with previous experimental published data, this suggests that the chemical characteristic of the nitrogen-containing bisphosphonates (N-BPs) is responsible for its biological effect and binding with hydroxyapatite surfaces.^[2,14,20,21]

XPS characterization

High-resolution XPS spectra were used after drying to verify the presence of adsorbate groups from bisphosphonate adsorption on titania surfaces in water. Samples immersed in bisphosphonate aqueous solutions with a concentration of 1 mM for 15 minutes and 2 hours were used to confirm the

surface modification of the titania substrates in a short time. The XPS findings for the overnight exposure were published elsewhere.^[13] Figure 3 presents the XPS high-resolution C1s, O1s, and N1s spectra for sputtered-deposited titania. The C1s signal exhibited four contributions at 285.0 eV from aliphatic carbon and contributions at higher binding energy, centered at 285.9 eV, 286.6 eV, and 288.8 eV, also from adventitious carbon, in agreement with previous work.^[16] O1s signal showed two contributions centered at 530.1 eV and 531.3 eV, which are oxidic oxygen from titanium dioxide and organic oxygen/hydroxyl groups, respectively. Finally, N1s spectra presented a single contribution at 400.2 eV, and a minor contribution from organic nitrogen species was also observed on C1s spectra at 285.9 eV.^[25,26]

C1s, O1s, and N1s high-resolution spectra for bisphosphonate species adsorbed on titania are presented in Figures 3 and 4. As bisphosphonic acid molecules have a similar composition due to the common $-\text{O}_3\text{P}-\text{C}(\text{OH})\text{R}-\text{PO}_3^-$ backbone and only differ in the respective substituent R, a difference in the spectra is expected mainly in the C1s and N1s signals. The full widths at half maximum (FWHM) of the peaks obtained from fitting can be found in the supplementary material. C1s high-resolution spectra of TiO_2/BP layers presented the same contributions observed on pristine titania. Centered at

286.2 eV, the contribution related to $\text{P}_2\text{C}^*\text{-O}$ moieties is characteristic of bisphosphonic acids as presented in Figure S3 for bulk etidronate.^[27] The decreased area related to carboxyl moieties on the TiO_2/ETI sample compared with the pristine titania surface is related to competitive adsorption, as observed for ODPa monolayers.^[16] No differences were observed with the increased immersion time, indicating that the surface rapidly reached saturation and that 15 m, 2 h, and 24 h may present similar behavior.

Figure 4 presented the O1s and the N1s high-resolution spectra of bisphosphonic acid layers adsorbed on titania after 2 hours of immersion. P2p high-resolution spectra were adjusted using an area ratio of 2:1 between $2\text{p}_{3/2}$ and $2\text{p}_{1/2}$ contributions due to the spin-orbit coupling, and the plot was omitted. All adsorbed bisphosphonates showed a $\text{P}2\text{p}_{3/2}$ binding energy of $133.3 (\pm 0.1)$ eV, this indicates a lack of differential surface charging during the measurements and that calibration based on positioning the C1s signal of hydrocarbonaceous carbon species at 285.0 eV was appropriate.^[28] As the samples were thoroughly rinsed with solvent after functionalization, the detected bisphosphonates were considered adsorbed on titania.

O1s high-resolution spectra showed three peaks for all titania samples/BP. Contributions were fitted based on the

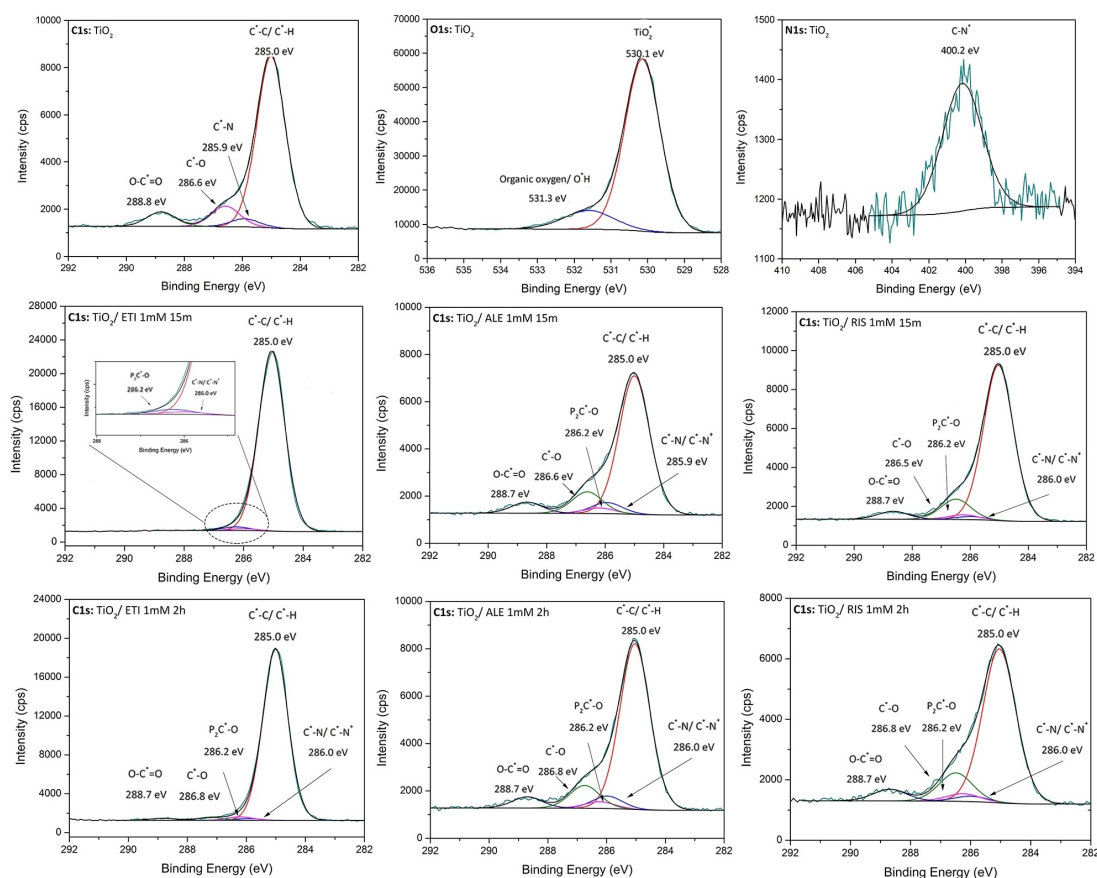


Figure 3. C1s, O1s, and N1s high-resolution spectra for sputtered-deposited titania; C1s high-resolution spectra of etidronic acid (ETI), alendronic acid (ALE), and risedronic acid (RIS) layers adsorbed on titania.

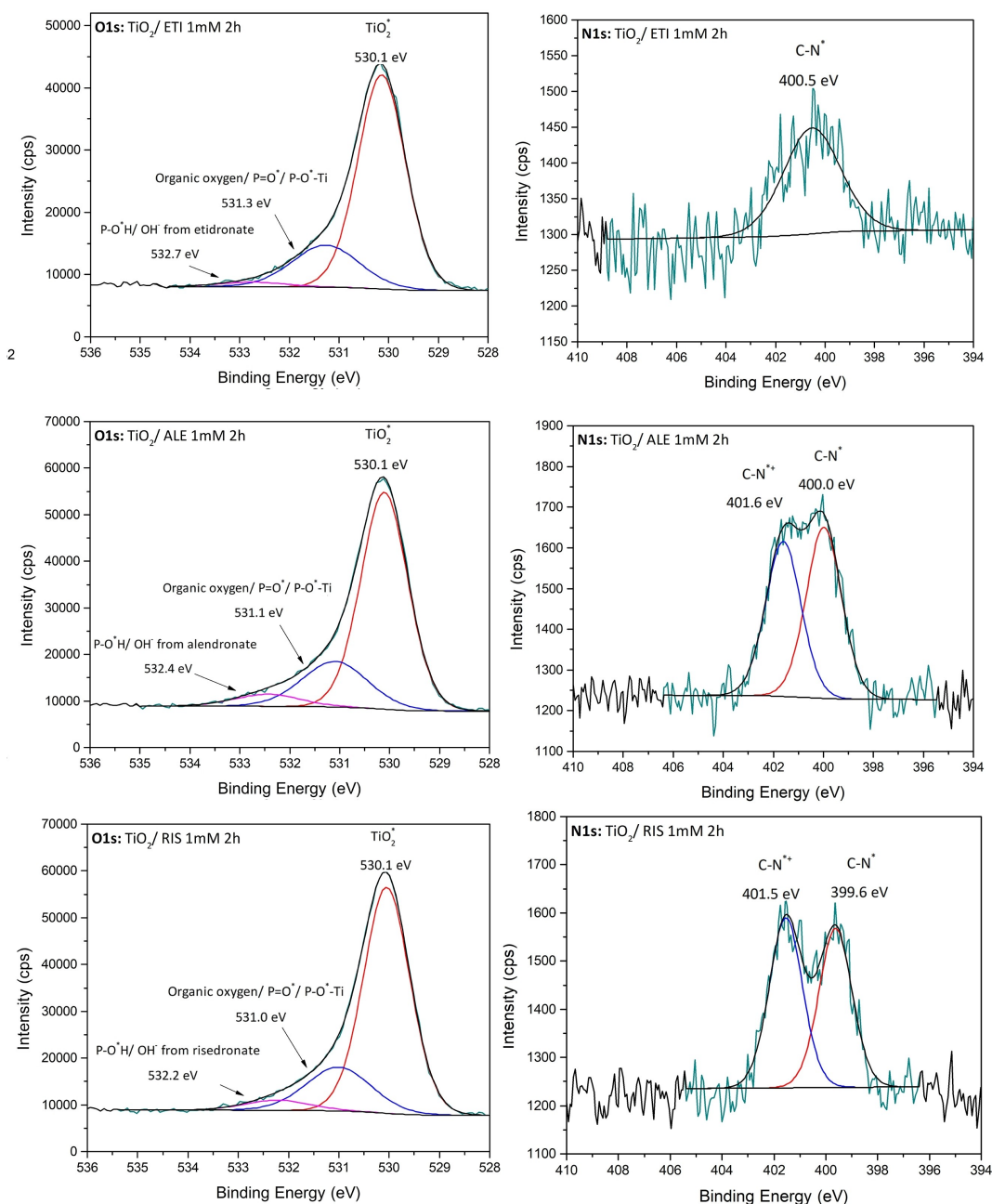


Figure 4. O1s and N1s XPS signals for etidronic acid (ETI), alendronic acid (ALE), and risedronic (RIS) adsorbed on titania.

approach previously published for bulk ODPA; as the molecule has a phosphonate group, the presence of P=O, P-O-H, and P-O-Ti groups would be expected for adsorbed bisphosphonates.^[16,25,29] Thus, the spectrum was fitted considering a third peak at higher binding energy from P-O*-H contribution, related to free phosphonic acid moieties. The peak around 530.1 eV is related to oxide species from titania substrate.^[30] The second peak is from organic oxygen, P=O*, and P-O*-Ti species around 531.1 eV and free/not adsorbed P-O*-H species around 532.4 eV.^[14,25,29] The formation of P-O-Ti may occur through a Ti⁺ and PO⁻ species, consistent

with DFT results. BPs can also protonate when exposed to Ti-OH groups, which leads to a condensation reaction, forming P-O-Ti and H₂O.

For the N1s signal, one contribution is expected from the alendronate and risedronate structure from the substituent R₂; however, along with the organic contribution of about 400 eV, the presence of nitrogen N1s peak centered at 401.6 eV was detected and attributed to positively charged nitrogen.^[30] Nitrogen species about 398 eV were not verified on sputtered-deposited titania, as presented in a previous study for rough rutile surfaces (R_a = 9.34 ± 0.2 nm).^[13] The same was true for

ammonium. These results reinforce that the surface chemistry of oxide surfaces influences the adsorption of nitrogen-containing bisphosphonates.^[12]

Although these differences compared with other XPS studies in the literature of BPs adsorbed on TiO₂, prior surface hydroxylation modifies the conformation of bisphosphonates.^[12,13] Consequently, our results may indicate a particularity of amorphous titania and BP adsorption. The composition of titania surfaces influences the point of zero charge (pzc). The pzc values of crystalline and amorphous titania are different on flat surfaces.^[31] Since the adsorption of BPs was done using HPLC quality water (pH 7), the surface had a charge close to zero, allowing the protonation of nitrogen groups during the adsorption.^[32,33] Some N-BPs are protonated at physiological pH.^[34] Further investigations must be performed to elucidate additional details and the influence of titania surface and chemistry on bisphosphonate adsorption.

To obtain details about bisphosphonate layer formation, we followed the procedure introduced by Goncalves *et al.*, the relative [P]/[Ti] concentration ratios normalized for a self-assembled monolayer of octadecylphosphonic acid (ODPA) on sputter-deposited titania were compared.^[16] Table 1 provides

$\{([P]/[Ti])/([P]/[Ti]_{ODPA\ SAM})\}$ values for different BP/titania adsorbates. Since they are smaller than the ones observed for a monophosphonate SAM even though a BP moiety contains two $-PO_3^-$ groups instead of one per ODPAs species, we inferred that all the titania/BP adsorbates are characterized by a lower area density of adsorption sites than the ODPAs SAMs.

Based on this table and XPS results, 15 minutes and 2 hours of immersion leads to an exposure of phosphonates moieties, which was also confirmed for overnight exposure.^[13] Such exposure influences properties such as water contact angle and zeta potential. Furthermore, a comparison of the normalized [P]/[Ti] ratio shows that the conformation of BPs on the titania surface is not strongly affected by the increase in immersion time. Finally, the ratio of N-BPs and etidronic acid is about 1.5. This was attributed to the fact that etidronic acid can adsorb only through two phosphonates groups. Nitrogen-containing BPs can interact through three different sites, leading to lower values of [P]/[Ti] as the nitrogen groups interact with hydroxyl groups on the titania surface forming N⁺ species, as detected by XPS.^[35] The interaction of nitrogen groups occupies a site that blocks a bond of another molecule. This idea is summarized in Figure 5.

Table 1. Normalized XPS signal intensity ratios for bisphosphonate samples adsorbed on TiO₂, based on an octadecylphosphonic acid monolayer (ODPA SAM) previously published.

Sample name	$\{([P]/[Ti])/([P]/[Ti]_{ODPA\ SAM})\}$
TiO ₂ /ETI 1 mM 15 m	1.30
TiO ₂ /ETI 1 mM 2 h	0.94
TiO ₂ /ALE 1 mM 15 m	0.59
TiO ₂ /ALE 1 mM 2 h	0.62
TiO ₂ /RIS 1 mM 15 m	0.62
TiO ₂ /RIS 1 mM 2 h	0.59
TiO ₂ /ODPA SAM	1.00

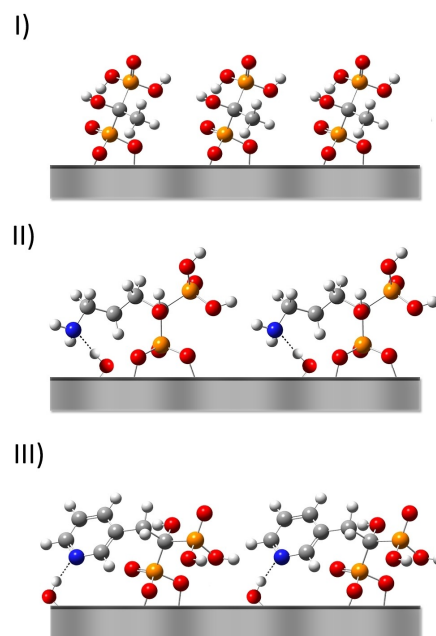


Figure 5. Representation of I) etidronic acid, II) alendronic acid, and III) risedronic acid molecules adsorbed on titania surface. Hydrogen atoms are represented in white, carbon in grey, oxygen in red, nitrogen in blue, and phosphorous in yellow.

Contact angle

Water contact angle measurements were performed to verify the modification of the surface wetting behavior due to bisphosphonate adsorption on titania surfaces. A spreading of water was reported for bisphosphonate layers due to the presence of phosphonates and nitrogen-containing groups.^[14,36,37] Our findings from water contact angle measurements are in Table 2.

The presence of $-PO_3H_2$ and $-NH_2$ groups provides a hydrophilic behavior on surfaces.^[4,12,13,36] Our results indicate that the titania surface is hydrophilic after the immersion in all the bisphosphonate solutions. XPS results show the presence of phosphonate and nitrogen groups on the surface after 15 minutes of thorough rinsing with water, a period that exceeds the contact time between the water droplet and the titania surface/BP. Thus, although the wetting behavior of the titania/BP surfaces is similar to that of pristine titania, we inferred that the WCA findings relate to BP adsorbate systems. The surface containing risedronate exhibited a slightly higher value,

Table 2. Water contact angle (WCA) for the studied layers.

Sample name	Water contact angle (°)
TiO ₂	11.4 ± 3.5
TiO ₂ /Alendronate	21.6 ± 2.6
TiO ₂ /Etidronate	15.1 ± 1.0
TiO ₂ /Risedronate	22.8 ± 2.0

possibly due to the pyridinium ring. This behavior was reported in previous work on rough surfaces.^[13]

Zeta potential measurements

Zeta potential measurements of bisphosphonate adsorbates are scarce. Electrokinetic assessments are performed only on hydroxyapatite particles or related particulate materials. Thus, the following results are the first that demonstrate BP/titania zeta potential measurements on a solid surface over a range of pH values. Smooth substrates were used to reduce the influence of roughness, as presented elsewhere.^[16]

The results from zeta potential measurements are displayed in Figure 6. For pristine titania, the same behavior depicted in a previous work was observed.^[16] The bisphosphonates exhibited increased zeta potential values compared to pristine titania with a decreased pH. In neutral pH, the phosphonate groups exist mainly as deprotonated groups (C-PO_3^{2-}) rather than $\text{C-PO}_3\text{H}_2$, leading to negative values for zeta potential at pH values around 6.7.^[23] This is consistent with the findings from MEP simulations, indicating that deprotonated phosphonic acid is predominant.

Although etidronate has the simplest structure of the investigated bisphosphonic acids, TiO_2/ETI curve is very similar to ODPa on titania, where the surface has more negative charge values than pristine titania, this indicates the presence of the adsorbates on the surface. Such values are attributed to unbonded P-OH, corroborated by XPS results.^[16] This is also confirmed by the MEP findings, as the etidronic acid molecule becomes more suitable for nucleophilic attacks after two deprotonations than in a neutral state.

As reported, the zeta potential of alendronate adsorbates has positive values for zeta potential on hydroxyapatite crystals at physiological pH, while the opposite occurs for risedronate.^[6] Despite this contrast, both presented similar biological efficacy at the same concentration. The surface containing alendronate has a curve similar to pristine titania; a similar behavior was

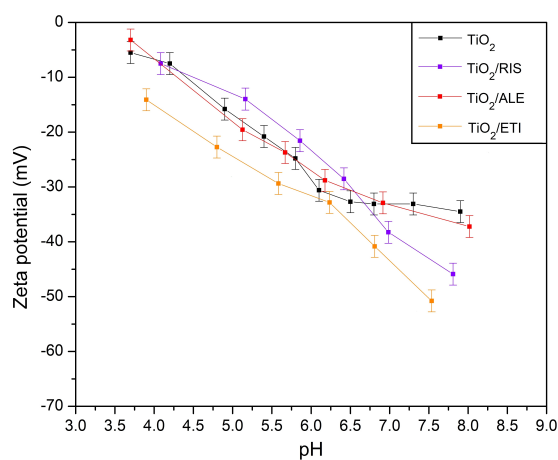


Figure 6. Zeta potential measurements of bisphosphonates adsorbed on TiO_2 .

reported for alendronate on the titania surface at pH 7.4.^[12] The presence of protonated amine plays an important role in balancing the deprotonated phosphonate. MEP validated such behavior. Moreover, different studies found that free alendronate has a charge equal to zero in acidic conditions due to the protonated amine and one deprotonated phosphonate. However, with the increase of the pH at physiological value, additional hydrogens leave the phosphonate leading to a negative liquid charge.^[20,22] As presented by XPS, approximately half of the amine groups are protonated. Consequently, the small decrease of the zeta potential compared with the pristine titania may occur due to the limited number of deprotonated phosphonates.

For risedronate, the presence of nitrogen influences the zeta potential only when pH is lower than 3. Deprotonation of phosphonates starts at pH 5 and reaches the maximum effect at pH greater than 10.^[23] Hence, the TiO_2/RIS curve becomes more negative after pH 6, near to etidronate. This is reinforced by the presence of P-OH moieties observed through XPS and the change of electrostatic potential from theoretical modeling.

Atomic force microscopy

Figure 7 contains topography images and the RMS of roughness. Peak heights can vary according to the adsorbate on the surface based on the scale bar. Samples showed a similar roughness value as the pristine substrate after adsorption of bisphosphonates, except for alendronic acid, which presented a slightly lower value. Due to the low roughness of substrate surface and the lack of data from bisphosphonates in the literature, the results are difficult to compare with other studies. Nonetheless, few studies present the change of roughness caused by bisphosphonic acid adsorption.

On hydroxyapatite (HA) surfaces, values can vary from 28.9 to 50.1 nm for pristine HA and etidronic acid adsorbed on HA, respectively.^[38] Smooth titania exhibited no significant change in surface roughness after adsorption of alendronic acid using different strategies. The reported values vary between 187 and

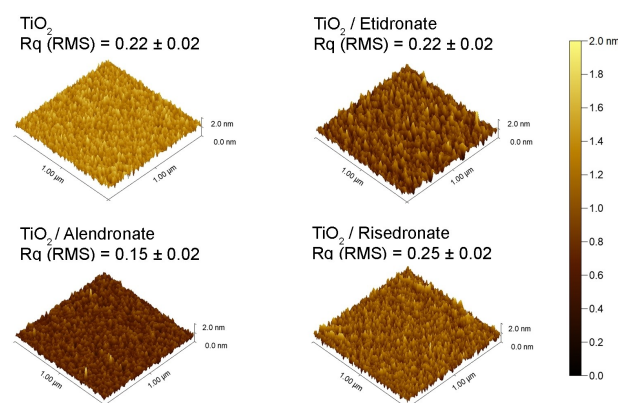


Figure 7. AFM images of bisphosphonates adsorbed on smooth titania.

175 nm for pristine and functionalized substrates, respectively.^[12]

As mentioned in the discussion of the XPS results, surface chemistry plays an important role in bisphosphonic acid adsorption. Thus, the surface topography may also affect the adsorption process. A smooth surface might favor an arrangement where the molecules follow the titania topography, as observed in octadecylphosphonic acid.^[16] A rough surface, especially hydroxyapatite, may approximate the molecules increasing the adsorption caused by the charge of bisphosphonic acids, thus leading to higher roughness values.^[6]

Conclusion

This work presents insights about changes in physicochemical aspects of bisphosphonate layers on titanium dioxide. The results help broaden the comprehension of BPs on titania surfaces through theoretical modeling and extensive surface characterization. The study demonstrated that pH and adsorption medium must be considered when dealing with these molecules. In the case of an aqueous medium, oxygen increases the chance of nucleophilic interactions, while nitrogen is more suitable for electrophilic attacks. The DFT results were corroborated by the XPS investigation, in which high-resolution N1s show protonated species on alendronate and risedronate. Besides this, it was demonstrated the formation of Ti–O–P bonds, consistent with the MEP results. XPS investigation demonstrated that exposed phosphonate moieties influence water contact angle and zeta potential; furthermore, the presence of additional groups leads to less dense layers of nitrogen-containing BPs compared with etidronic acid. Water contact angle measurements confirmed that these groups lead to more hydrophilic surfaces, indicating that all functionalized samples remained with a low WCA. For zeta potential measurements, the particularity of each structure was discussed on a solid surface, considering a pH range for the first time. For etidronate, the prevalence of negative charges of unbounded P–OH leads to more negative values of zeta potential. Despite exhibiting free phosphonates, alendronate has a protonated amine which partially balances the charge leading to values close to pristine TiO₂. On the other hand, the influence of the nitrogen group is reduced on risedronate, because protonation occurs only at a pH lower than 3. Thus, at pH higher than 6, zeta potential indicates negative values, forced by free P–OH groups, which start the protonation close to pH 5. After adsorption of bisphosphonates, the titania surface remains smooth, suggesting that the molecules may be affected by substrate roughness and surface chemistry. As complementary works, we recommend quantitative measurements of the adsorbed amount of BP and also the stability of BP layers, and the determination of adsorptions curves of bisphosphonic acids with deeper computational modeling (such as adsorption energy calculations of the BP's + substrate system). The use of bioactive molecules adsorbed on smooth surfaces was revealed as a suitable strategy to provide a deeper understanding of the physicochemical aspects of these molecules, particularly when allied with modeling. Once the surface is well characterized,

the next step is to understand how surface properties influence biological performance.

Supporting Information Summary

The supporting information comprises details of sample preparation and experimental details for data acquisition. Bisphosphonates modeling in a vacuum is also presented, as well XPS measurements of bulk etidronate, and FWHM of XPS analysis.

Acknowledgements

The authors are grateful to the São Paulo Research Foundation (FAPESP) for the financial support through the grants 2019/13100-0, 2018/07520-3, and 2019/09431-0. Marina Honorato Cardoso for critical reading. Dirk Salz assisted with sputtering deposition, and Thorben Brenner supported zeta potential measurements. Open Access funding enabled and organized by Projekt DEAL.

Conflict of Interest

The authors declare no conflict of interest.

Data Availability Statement

Research data are not shared.

Keywords: adsorption · bisphosphonate · DFT · surface characterization · titanium dioxide

- [1] S. A. Holstein, D. M. Cermak, D. F. Wiemer, K. Lewis, R. J. Hohl, *Bioorg. Med. Chem.* **1998**, *6*, 687–694.
- [2] C. Chen, M. Xia, L. Wu, C. Zhou, F. Wang, *J. Mol. Model.* **2012**, *18*, 4007–4012.
- [3] M. T. Drake, B. L. Clarke, S. Khosla, *Mayo Clin. Proc.* **2008**, *83*, 1032–1045.
- [4] L. Rojo, B. Gharibi, R. McLister, B. J. Meenan, S. Deb, *Sci. Rep.* **2016**, *6*, 1–10.
- [5] B. Peter, D. P. Pioletti, S. Laib, B. Bujoli, P. Pilet, P. Janvier, J. Guicheux, P. Y. Zambelli, J. M. Boulter, O. Gauthier, *Bone* **2005**, *36*, 52–60.
- [6] G. H. Nancollas, R. Tang, R. J. Phipps, Z. Henneman, S. Gulde, W. Wu, A. Mangood, R. G. G. Russell, F. H. Ebetino, *Bone* **2006**, *38*, 617–627.
- [7] D. Sidane, H. Rammal, A. Beljebbar, S. C. Gangloff, D. Chicot, F. Velard, H. Khireddine, A. Montagne, H. Kerdjoudj, *Mater. Sci. Eng., C* **2017**, *72*, 650–658.
- [8] A. Arifin, A. B. Sulong, N. Muhamad, J. Syarif, M. I. Ramli, *Mater. Des.* **2014**, *55*, 165–175.
- [9] L. D. Trino, E. S. Bronze-Uhle, A. George, M. T. Mathew, P. N. Lisboa-Filho, *Colloids Surf., A* **2018**, *546*, 168–178.
- [10] E. S. Bronze-Uhle, L. F. G. Dias, L. D. Trino, A. A. Matos, R. C. De Oliveira, P. N. Lisboa-Filho, *Colloids Surf., A* **2019**, *564*, 39–50.
- [11] F. López-Huerta, B. Cervantes, O. González, J. Hernández-Torres, L. García-González, R. Vega, A. L. Herrera-May, E. Soto, *Mater.* **2014**, *7*, 4105–4117.
- [12] D. Zheng, K. G. Neoh, E. T. Kang, *J. Colloid Interface Sci.* **2017**, *487*, 1–11.
- [13] E. S. Bronze-Uhle, L. F. G. Dias, L. D. Trino, A. A. Matos, R. C. De Oliveira, P. N. Lisboa-Filho, *Surf. Coat. Technol.* **2019**, *357*, 36–47.
- [14] Ž. Petrović, A. Šarić, I. Despotović, J. Katić, R. Peter, M. Petrić, M. Petković, *Mater.* **2020**, *13*, DOI 10.3390/ma13143220.
- [15] M. Geetha, A. K. Singh, R. Asokamani, A. K. Gogia, *Prog. Mater. Sci.* **2009**, *54*, 397–425.

- [16] L. F. Gonçalves Dias, S. Stamboroski, M. Noeske, D. Salz, K. Rischka, R. Pereira, M. do C. Mainardi, M. H. Cardoso, M. Wiesing, E. S. Bronze-Uhle, R. B. Esteves Lins, P. N. Lisboa-Filho, *RSC Adv.* **2020**, *10*, 39854–39869.
- [17] K. Suttiponparnit, J. Jiang, M. Sahu, S. Suvachittanont, T. Charinpanitkul, P. Biswas, *Nanoscale Res. Lett.* **2011**, *6*, 1–8.
- [18] F. Borghi, V. Vyas, A. Podestà, P. Milani, *PLoS ONE* **2013**, *8*, 1–14.
- [19] L. Vidyasagar, P. Apse, *Baltic Dent. Maxillofac. J.* **2004**, *6*, 51–54.
- [20] D. Fernández, J. Ortega-Castro, J. Frau, *Appl. Surf. Sci.* **2017**, *392*, 204–214.
- [21] M. H. Ri, Y. M. Jang, U. S. Ri, C. J. Yu, K. Il Kim, S. U. Kim, *J. Mater. Sci.* **2018**, *53*, 4252–4261.
- [22] J. Ke, H. Dou, X. Zhang, D. S. Uhagaze, X. Ding, Y. Dong, *J. Pharm. Anal.* **2016**, *6*, 404–409.
- [23] D. A. Bedoya, C. Vasti, R. Rojas, C. E. Giacomelli, *Appl. Clay Sci.* **2017**, *141*, 257–264.
- [24] J. Melin, F. Aparicio, V. Subramanian, M. Galván, P. K. Chattaraj, *J. Phys. Chem. A* **2004**, *108*, 2487–2491.
- [25] C. Theile-Rasche, M. Wiesing, S. Schwiderek, M. Noeske, G. Grundmeier, *Appl. Surf. Sci.* **2020**, *513*, 145701.
- [26] J. Landoulsi, M. J. Genet, C. Richard, K. El Kirat, S. Pulvin, P. G. Rouxhet, *Journal of Colloid and Interface Science* **2008**, *318*, 278–289.
- [27] F. Gao, P. M. A. Sherwood, *Surf. Interface Anal.* **2013**, *45*, 742–750.
- [28] P. E. B. K. D. Moulder, J. F. Stickle, W. F. Sobol, *Handb. X-Ray Photoelectron Spectrosc.* **1993**.
- [29] V. Zoulalian, S. Zürcher, S. Tosatti, M. Textor, S. Monge, J. J. Robin, *Langmuir* **2010**, *26*, 74–82.
- [30] G. Beamson, D. Briggs, *J. Chem. Educ.* **1993**, *5*, 778–778.
- [31] M. Kosmulski, *Adv. Colloid Interface Sci.* **2002**, *99*, 255–264.
- [32] T. Hanawa, *J. Periodontal Implant Sci.* **2011**, *41*, 263–272.
- [33] P. Sriprang, S. Wongnawa, O. Sirichote, *J. Sol-Gel Sci. Technol.* **2014**, *71*, 86–95.
- [34] D. Fernández, J. Ortega-castro, J. Frau, *Appl. Surf. Sci.* **2018**, *392*, 204–214.
- [35] J. P. Spatz, M. Möller, M. Noeske, R. J. Behm, M. Pietralla, *Macromol.* **1997**, *30*, 3874–3880.
- [36] S. R. Cicco, D. Vona, G. Leone, E. De Giglio, M. A. Bonifacio, S. Cometa, S. Fiore, F. Palumbo, R. Ragni, G. M. Farinola, *Mater. Sci. Eng., C* **2019**, *104*, 109897.
- [37] A. H. Almuqrin, S. Wjhi, F. Aouaini, A. Ben Lamine, *J. Mol. Liq.* **2020**, *310*, 113230.
- [38] M. Othmani, A. Aissa, C. G. Bac, F. Rachdi, M. Debbabi, *Appl. Surf. Sci.* **2013**, *274*, 151–157.

Submitted: January 23, 2022

Accepted: April 7, 2022